Thermochromatium tepidum Photoactive Yellow Protein/Bacteriophytochrome/Diguanylate Cyclase: Characterization of the PYP Domain†

John A. Kyndt, John C. Fitch, Terry E. Meyer, and Michael A. Cusanovich*

Department of Biochemistry and Molecular Biophysics, University of Arizona, Tucson, Arizona 85721

Received December 14, 2004; Revised Manuscript Received January 19, 2005

ABSTRACT: The purple phototrophic bacterium, *Thermochromatium tepidum*, contains a gene for a chimeric photoactive yellow protein/bacteriophytochrome/diguanylate cyclase (Ppd). We produced the *Tc. tepidum* PYP domain (Tt PYP) in *Escherichia coli*, and found that it has a wavelength maximum at 358 nm due to a Leu46 substitution of the color-tuning Glu46 found in the prototypic *Halorhodospira halophila* PYP (Hh PYP). However, the 358 nm dark-adapted state is in a pH-dependent equilibrium with a yellow species absorbing at 465 nm ($pK_a = 10.2$). Following illumination at 358 nm, photocycle kinetics are characterized at pH 7.0 by a small bleach and red shift to what appears to be a long-lived cis intermediate (comparable to the I_2 intermediate in Hh PYP). The recovery to the dark-adapted state has a lifetime of ∼4 min, which is approximately 1500 times slower than that for Hh PYP. However, when the Tt PYP is illuminated at pH values above 7.5, the light-induced difference spectrum indicates a pH-dependent equilibrium between the I_2 intermediate and a red-shifted 440 nm intermediate. This equilibrium could be responsible for the sigmoidal pH dependence of the recovery of the dark-adapted state ($pK_a = 8.8$). In addition, the light-induced difference spectrum shows that, at pH values above 9.3, there is an apparent bleach near 490 nm superimposed on the 358 and 440 nm changes, which we ascribe to the equilibrium between the protonated and ionized dark-adapted forms. The L46E mutant of Tt PYP has a wavelength maximum at 446 nm, resembling wild-type Hh PYP. The kinetics of recovery of L46E following illumination with white light are slow (lifetime of 15 min at pH 7), but are comparable to those of wild-type Tt PYP. We conclude that Tt PYP is unique among the PYPs studied to date in that it has a photocycle initiated from a dark-adapted state with a protonated chromophore at physiological pH. However, it is kinetically most similar to *Rhodocista centenaria* PYP (Ppr) despite the very different absorption spectra due to the lack of E46.

Photoactive yellow protein (PYP)[1] is a small cytoplasmic blue light-absorbing sensory protein discovered in *Halorhodospira* (also known as *Ectothiorhodospira*) *halophila* (*1*, *2*). More recently, it has been found that PYP also can be part of larger multidomain proteins (*3*). Several publications have presented PYP as the structural prototype for the PAS domain family (*4*, *5*). PAS domains are signaling modules that sense a wide range of stimuli, e.g., light, oxygen, redox potential, and a wide variety of small molecules (*6*−*8*). On the basis of homology, kinetics of recovery following photoexcitation, and presumed function, the PYPs found to date can be classified in four groups (*9*).

The first group comprises the PYPs found in the halophilic organisms *Hr. halophila*, *Rhodothallasium* (also known as *Rhodospirillum*) *salexigens*, and *Halochromatium* (also known as *Chromatium*) *salexigens* (*10*, *11*). All three have similar kinetics, and the photocycle of Hh PYP is by far the best studied of all PYPs. In general, the dark-adapted state of Hh PYP absorbs light with a maximum at 446 nm, and a laser flash initiates a trans−cis isomerization of the anionic *p*-hydroxycinnamic acid chromophore, concomitant with conversion of the dark-adapted state P into I_0 (1.9 ps) and subsequently into $I_0^{\ddagger}$ (220 ps) both absorbing at 510 nm (*12*−*14*). $I_0^{\ddagger}$ decays into the red-shifted I_1 intermediate in ∼3 ns ($\lambda_{max} = 465$ nm). In ∼500 μs, I_1 decays to I_1' which has the ionized chromophore exposed to the solvent (*15*). Fast protonation by the solvent results in the blue-shifted I_2 ($\lambda_{max} = 350$ nm). Recently, evidence was provided for this $I_1'-I_2$ equilibrium with a pK_a of 8.2 for the E46Q Hh PYP mutant and ∼11 for WT Hh PYP (*15*). A major conformational change in the protein after ∼1.5 ms forms the I_2' intermediate (*14*, *16*), which decays to the dark-adapted state with a lifetime of ∼160 ms, although slower times have also been reported.

The second group contains the single domain PYP's from two *Rhodobacter* species: *Rhodobacter sphaeroides* (*17*, *18*) and *Rhodobacter capsulatus* (*3*, *19*). In both cases, the PYP has an additional absorption maximum in the UV−vis region at neutral pH, at 360 nm for *Rb. sphaeroides* PYP and at

† This work was supported by Grant GM66146 from the National Institutes of Health.

* To whom correspondence should be addressed: Department of Biochemistry and Molecular Biophysics, University of Arizona, 1041 E. Lowell St., Tucson, AZ 85721. Telephone: (520) 621-7533. Fax: (520) 621-6603. E-mail: cusanovi@u.arizona.edu.

[1] Abbreviations: PAS, acronym formed from the names of the first three proteins recognized as sharing this sensor motif (periodic clock protein of *Drosophila*, aryl hydrocarbon receptor nuclear translocator of vertebrates, and single-minded protein of *Drosophila*); WT, wild-type; PYP, photoactive yellow protein; Ppd, PYP/phytochrome/diguanylate cyclase; PCR, polymerase chain reaction; Bph, bacteriophytochrome; IPTG, isopropyl β-D-thiogalactoside.

10.1021/bi047373n CCC: $30.25
Published on Web 03/04/2005

375 nm for *Rb. capsulatus* PYP. The photocycle of the *Rhodobacter* PYPs is completed ~100 times faster than that of the first group. The relatively fast kinetics suggest that the *Rhodobacter* PYPs sense a higher light intensity than Hh PYP, since this would be required to achieve a significant steady-state concentration of the signaling state.

In the third group, with a single representative from *Rhodocista* (also known as *Rhodospirillum*) *centenaria*, the PYP is actually the N-terminal domain of a larger protein called Ppr (*3*). In Ppr, the central domain is a bacteriophytochrome (Bph), which is followed by a C-terminal histidine kinase domain. Recent investigation showed that the photocycle of the recombinant PYP domain is ~3 orders of magnitude slower than that of the prototypic Hh PYP, suggesting that it senses much lower light intensities than either of the first two groups (*3*). The Ppr holoprotein, reconstituted with both chromophores, has approximately the same kinetics for the PYP photocycle as in the Ppr PYP domain, and the Bph chromophore is bleached at 702 nm rather than being red-shifted as in other phytochromes (*9*). The Bph recovers in a biphasic fashion with time constants of 2.5 min (like the Ppr PYP domain) and 1.6 h (not observed with the Ppr PYP domain recovery). It has been shown that Ppr is involved in regulation of the gene for a polyketide synthase similar to chalcone synthase whereby expression is inhibited 2-fold when Ppr is illuminated and presumably bleached in either the PYP domain, the Bph domain, or both (*3*). The cognate response regulator has not yet been identified.

Recently, we reported the discovery of a *ppd* gene from the genome of *Thermochromatium tepidum* (Integrated Genomics), which represents a fourth structural and functional form, that encodes a PYP homologue fused to a Bph domain which is followed by a third domain (*9*). This gene structure resembles that of the *Rc. centenaria ppr*; however, the third domain in the case of the *Tc. tepidum* gene shows homology (~38%) to the GGDEF/EAL family of diguanylate cyclases/phosphodiesterases instead of the histidine kinases. We therefore named it *Tc. tepidum* Ppd (PYP/phytochrome/diguanylate cyclase). We now report characterization of the *Tc. tepidum* PYP domain. We confirmed that this PYP has a substitution of Leu for the color-tuning Glu46. Nevertheless, it has a photocycle that is similar to those of the other species of PYP, but in this case, the photocycle is initiated from a dark-adapted state with a protonated chromophore absorbing at 358 nm.

MATERIALS AND METHODS

Bacterial Cultures. Tc. tepidum was kindly provided by M. Madigan (Southern Illinois University, Carbondale, IL). The culture was grown as described previously (*20*).

Cloning and Mutagenesis. PCR was performed to isolate the first 378 bp of the gene encoding Ppd of *Tc. tepidum*. The forward and reverse primers were designed with NdeI and HindIII restriction sites, respectively, based upon the genome sequence determined by Integrated Genomics (Chicago, IL). After the PCR fragment had been digested with NdeI and HindIII restriction enzymes, it was ligated into the predigested pET20b vector. The gene was cloned under control of the T7 promoter and in frame with the His tag region of the pET20b vector, resulting in pET20b(TtepPYP). This construct allowed us to express the PYP domain as a single protein with a C-terminal His tag. The pET20b vector introduces a seven-amino acid linker (KLAAALE) between the end of the PYP domain and the His tag (six His residues).

Cotransformation of pET20b(TtepPYP) with the previously described biosynthetic plasmid pACYC(TALpCL) (*21*) resulted in an *Escherichia coli* BL21(DE3) strain which was able to produce holo-Tt PYP. The expression culture was grown at 30 °C and induced with 1 mM IPTG at an OD_{600} of 0.7. After overnight growth (~16 h), the cells were harvested by centrifugation, resuspended in 20 mM Tris-HCl (pH 7.5) with 100 mM NaCl, and lysed with an automated French press. The Tt PYP was purified from the crude cell lysate with TALON resin (BD Biosciences Clontech, Palo Alto, CA) which has a high affinity for His-tagged proteins. The purification was performed in batch as described by the manufacturer, and the protein eluted with 200 mM imidazole. Since the Tt PYP was only ~60% pure after this step, we performed a size exclusion purification on a Superdex 75 column using the ÄKTA Explorer (Amersham Biosciences) FPLC system. The protein was ~80% pure after this step, and a combination of SDS−PAGE and mass spectrometry showed that most of the contamination was due to the presence of apo-PYP. The purity was estimated from the 280 nm to 358 nm ratio in the absorption spectrum, suggesting there was ~20% apo-PYP. An additional Q-Sepharose ion exchange step did not improve the purity of the sample. The recombinant protein was used for additional characterization without removal of the His tag.

The L46E mutant of *Tc. tepidum* PYP was created using the Quick Change PCR mutagenesis kit (Stratagene). The following primers were used: TTCTACAGCCGCGCCGAAGTGGACCTTG and complement as the reverse primer. The mutated bases are underlined. The PCR was as described previously (*19*). The mutant protein was produced and purified as described above for the wild type, with the difference being that the sample was completely pure after the size exclusion step. No evidence for apo-PYP or other contaminants could be found in the mass spectrometry analysis.

Mass Spectrometry. The mass spectrometry experiments with both WT Tt PYP and L46E were performed at the Chemistry Department Mass Spectrometry Facility at the University of Arizona. Samples (10 μM) were in 5 mM Tris-HCl and were analyzed with ESI-MS, preceded by an HPLC separation. The WT Tt PYP sample exhibited a significant mass of 15 974 Da as well as the expected mass of 16 122 Da for the holo-PYP domain plus a His tag. The mass of 15 974 Da corresponds to the theoretical mass of the apo-Tt PYP domain. L46E exhibited only a single band with a mass of 16 137 Da which corresponds well to the theoretical mass of 16 138.1 Da for the mutated holo domain.

UV−Vis and Time-Resolved Laser Spectroscopy. Absorption spectra were obtained with a CARY 300 spectrophotometer. All studies were carried out in a universal buffer (2 mM CAPS, CHES, TAPS, HEPES, MES, sodium citrate and 1 mM PIPES), unless otherwise indicated. In the steady-state recovery experiments with the L46E mutant, the protein was first bleached by being exposed to a tungsten lamp (60 W) for 2 min, and subsequently, the recovery was measured in the dark in the CARY spectrophotometer. Some experiments were carried out with a 410 nm short band-pass filter

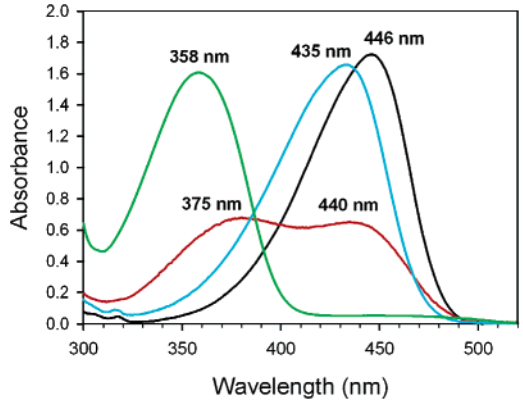

FIGURE 1: UV−vis absorption spectra of four types of PYP at pH 7.0: *Hh. halophila* PYP in black, *Rb. capsulatus* PYP in red, *Rc. centenum* PYP domain in cyan, and the *Tc. tepidum* PYP domain in green. There is a significant absorbance background in the *Tc. tepidum* PYP spectrum which could be due to aggregation and light scattering (see the text).

to excite only the 446 nm form. Absorbance changes were measured over a 40−120 min time range, and the kinetic data were fit using OLIS software (K-Fit, Bogart, GA).

In the recovery experiment with WT Tt PYP, samples were illuminated for 20 s with a 150 W Xe arc lamp to obtain a stronger signal. The absorbance changes during recovery were measured in the CARY spectrophotometer on a 2−10 min time scale. To obtain difference spectra, the spectrophotometer was used in the wavelength scanning mode and samples were taken with 6 s intervals.

The laser flash photolysis apparatus and data analysis protocol for the 365, 445, and 480 nm excitation were as described previously (*2*, *22*).

RESULTS AND DISCUSSION

Cloning and Spectral Characterization of Tc. tepidum PYP. We cloned the PYP domain (first 378 bp) of the Tt *ppd* and verified that it has the correct DNA sequence as originally determined by Integrated Genomics. Wild-type Tt PYP has a Leu at position 46 which is a Glu in Hh PYP in the equivalent position. This is of interest since Glu46 together with Tyr42 has been shown to be hydrogen-bonded to the phenolate oxygen of the chromophore (*23*) and Glu46 plays a significant role in color-tuning of Hh PYP (*24*). Therefore, the presence of Leu in WT Tt PYP was expected to render the protein colorless since the chromophore should absorb light in the UV rather than in the blue at pH 7.0. To verify that this is the case, we attached a His tag to the Tt *pyp* gene fragment and expressed it in *E. coli* along with the two biosynthetic enzymes (from *Rb. capsulatus*; *21*). The resulting recombinant protein has an absorption maximum at 358 nm. In Figure 1, the Tt PYP absorption spectrum is compared with that of the three other PYP classes at pH 7.0. Tt PYP (in green) has the most blue-shifted absorption maximum of all WT proteins found to date. Note that the E46A mutant of Hh PYP has an absorption maximum at 365 nm at pH 7.0 (24). However, as the pH is increased, Tt PYP, as with the E46A mutant of Hh PYP, absorbs light in the vicinity of 465 nm (see the Tt PYP spectra in Figure 2A). The pK_a for this transition in Tt PYP is 10.2 as shown in Figure 2B. The 358 nm to 465 nm transition is reversible below pH 10.4 (if performed quickly) and has an isosbestic

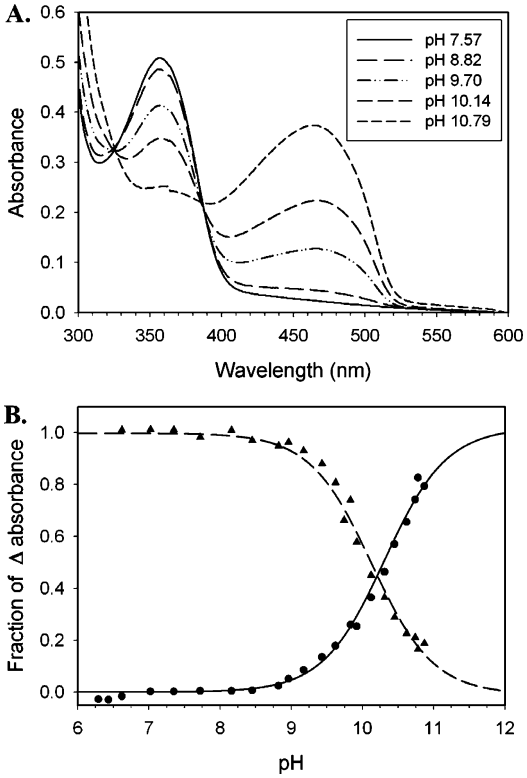

FIGURE 2: (A) Absorption spectra of WT *Tc. tepidum* PYP in universal buffer at different pH values. Above pH 10, the predominant form has an absorption maximum at 465 nm, resembling the E46A Hh PYP mutant. The background absorbance, presumably due to aggregation, also increases with an increase in pH. (B) Plot of the pH titration of Tt PYP. The absorbance was measured at 450 nm (●) and 360 nm (▲). The two plots were fit with the Henderson−Hasselbach equation, resulting in pK_a values of 10.2 and 10.1, respectively (n = 1 for both).

point at 388 nm, although above that pH, hydrolysis of the chromophore rapidly commences and interferes with the measurements. As can be seen from Figure 2A, there is an increase in background absorbance with increasing pH, presumably due to aggregation of the protein and consequent light scattering. This is most significant below 320 nm, but it can also explain why the 358 nm absorbance does not appear to reach the baseline at higher pH. This apparent aggregation effect, in addition to the presence of apo-PYP, contributes to the high 280 nm to 358 nm ratio of 1.35 (at pH 7.0). At this point, it is not certain if the presumed protein aggregation is due to apo-PYP, holo-PYP, or both. However, when the sample was centrifuged at 14 000 rpm for 10 min, a small fraction of the aggregate precipitated out, but the 280 nm to 465 nm ratio did not change significantly. This suggests that both apo- and holo-PYP are forming the aggregate.

The chromophore in Hh PYP has a pK_a at or below 2.8, where the protein denatures and hydrolysis of the chromophore begins (*1*). The shift in pK_a compared to that of the chromophore in solvent (which is near 9) is thought to be due to the formation of a hydrogen bond between the E46 carboxylic acid group and the ionized chromophore hydroxylate, which is broken when the protein denatures. In the absence of E46, however, as in the E46Q and E46A mutants of Hh PYP, there is a pH-dependent equilibrium between the normal ionized dark-adapted state (P, λ_{max} = 462 nm) and the protonated form of the chromophore inside

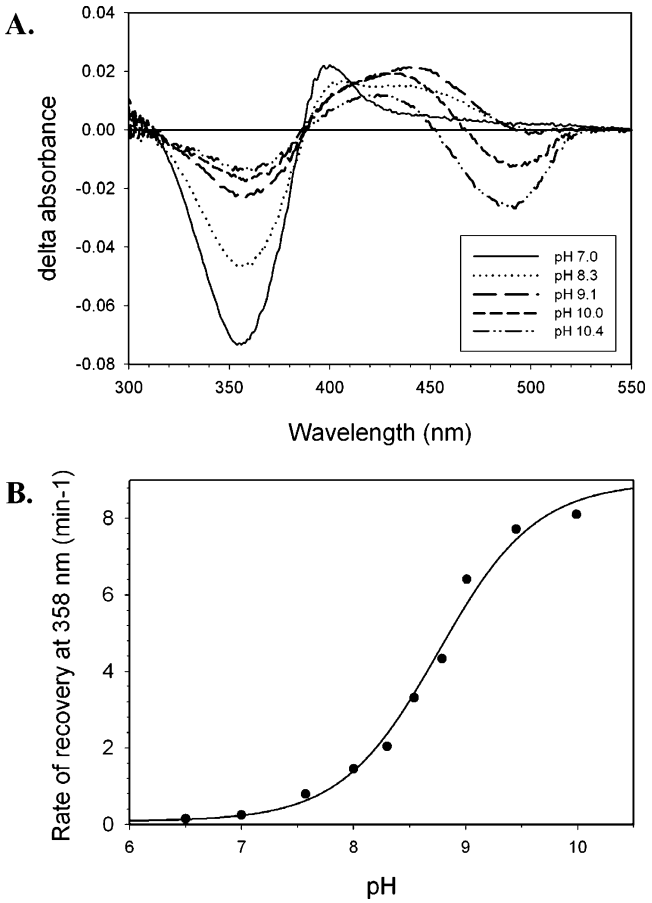

FIGURE 3: (A) Light minus dark difference spectra taken immediately after illumination with white light from a Xe arc lamp for 20 s. The spectra were taken at pH 7.0, 8.3, 9.1, 10.0, and 10.4. (B) Plot of the rate constant for recovery of WT Tt PYP at 358 nm after white light illumination as a function of pH. There is an at least 30-fold increase in recovery rate from pH 7.0 to 10.0. Measurements above pH 10.5 were impaired by hydrolysis of the chromophore. The plot was fit to a curve with a pK_a of 8.8 (n = 1).

the protein (P_{BL}), which absorbs near 350 nm (*15*, *24*, *25*). In those cases, the chromophore inside the protein has a pK_a closer to that in solvent (pK_a values of 4.8 and 7.9 for E46Q and E46A, respectively) and considerably higher than that for acid denaturation, which is not significantly altered by mutagenesis. The equilibrium we observe in Tt PYP is similar to this $P-P_{BL}$ equilibrium, where P is the dark-adapted state with an ionized chromophore (λ_{max} = 465 nm) and P_{BL} is the dark-adapted state in which the chromophore is protonated (λ_{max} = 358 nm). However, the pK_a of 10.2 is higher than that for the free chromophore, which might be a result of the chromophore residing in a more hydrophobic environment (due to the Leu46 substitution).

Photoactivity of Tc. tepidum PYP. When illuminated with white light from a Xe arc lamp (for 20 s), Tt PYP shows a small bleach at 358 nm and a red shift. This can be seen in the difference spectrum at pH 7.0 as a decrease at 358 nm and an increase in absorbance with a maximum at 395 nm (Figure 3A). On the basis of the relative amplitudes and separation of the 358 and 395 nm peaks, we estimate the wavelength maximum of the product formed by illumination to be around 368 nm. As a consequence of less than 100% conversion under steady-state conditions and the spectral overlap of the 358 nm species with the product, the maximum bleach at 358 nm is only ~30% of the pre-illumination absorbance. The photoproduct has a lifetime of ~4.1 min (k = 4.1 × 10^{-3} s^{-1}). In addition, the absorbance increase at 395 nm as compared to the absorbance decrease at 358 nm suggests that the intermediate species, which absorbs at 368 nm, has an extinction coefficient approximately half that of the 358 nm dark-adapted species. The red shift of ~10 nm upon illumination of Tt PYP is indicative of a trans−cis isomerization of the chromophore as shown for Hh PYP where the photoreversal of I_2 (cis state) to the dark-adapted state (trans state) was investigated (*26*, *27*). More importantly, our spectra are in agreement with the observation that the extinction coefficient of the trans form is larger than for the cis intermediate (*26*, *27*). Thus, we conclude that the 358 nm P_{BL} form has the protonated chromophore in a trans conformation in the folded protein. Following illumination, this is converted into the red-shifted I_2 intermediate which has the chromophore in the protonated cis conformation. A deprotonated cis chromophore would be expected to be more significantly red-shifted (see below).

The recovery kinetics of I_2 are highly pH dependent, with a more than 30-fold increase between pH 7.0 and 10 (Figure 3B). The pH profile for recovery of Tt PYP was fitted with a pK_a of 8.8 (n = 1). This pK_a is similar to that for the free chromophore (pK_a ~ 9) and for the pK_a values for the recovery rate constants of the E46Q and E46A mutants of Hh PYP (*15*, *24*, *25*). Since Tt PYP is lacking E46, this is not unexpected, and we believe that the pK_a of 8.8 is due to deprotonation of the solvent-exposed I_2 chromophore. This will be further discussed below.

pH-Dependent Equilibrium between I_2 and a 440 nm Form. When the pH dependence of the light-induced difference spectrum was investigated (Figure 3A), we found that at higher pH values (>7.5) there is formation of an additional red-shifted species at the expense of the I_2 intermediate (compare difference spectra at pH 7.0, 8.3, and 9.1 in Figure 3A). The increase in absorption is at 440 nm, although the real maximum might be slightly more to the red, which is masked by spectral overlap with I_2. The kinetics for decay of the 440 nm intermediate at pH 9.1 (τ = 10.4 s) correlate well with the recovery at 358 nm at pH 9.0 (τ = 9.1 s). The observation that the magnitude of the transient 440 nm species increases with an increase in pH while that of the I_2 species decreases indicates that there is a pH-dependent equilibrium between this new species and the I_2 seen at lower pH and they both decay with essentially the same rate constant.

A similar pH-dependent equilibrium was previously found between the I_1' and I_2 intermediates for the WT Hh PYP and its E46Q mutant (*15*). The I_1 intermediate is in the cis conformation and is red-shifted relative to the dark-adapted state, but the phenolate is still hydrogen-bonded to the protein. It is the chromophore C9 carbonyl that has rotated (~170° relative to the plane of the aromatic ring) in the trans to cis conversion (*28*). The I_1' intermediate also has a deprotonated cis chromophore which is presumably no longer hydrogen-bonded by the protein, but instead, the phenolate appears to have become solvent-exposed (*15*). Thus, I_1' is thought to have the same chromophore conformation as the I_2 intermediate and can be considered an ionized form of I_2, although this remains to be proven. By analogy to Hh PYP, the transient 440 nm species which we observe presumably

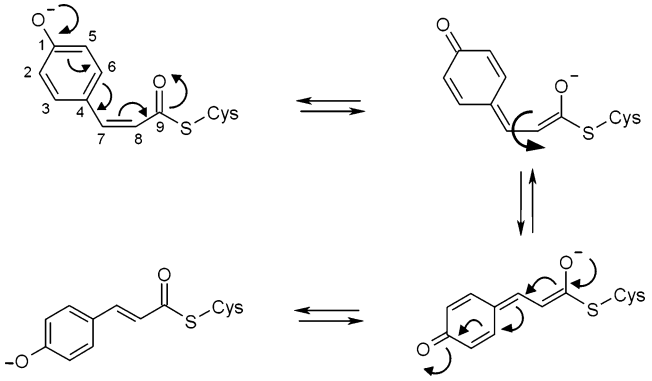

FIGURE 4: Tautomeric structures of the *p*-hydroxycinnamic acid chromophore attached to Cys69. An electron rearrangement starting at the phenolate oxygen turns the C7−C8 double bond into a single bond which facilitates formation of the trans isomer. A subsequent electron rearrangement forms the trans ionized chromophore which is present in the dark-adapted state.

also has a deprotonated cis chromophore. According to Kort et al. (*29*), the ionized form of the chromophore should have a wavelength maximum red-shifted by 75 nm from that of the protonated form. If the I_2 form of Tt PYP absorbs in the vicinity of 368 nm, we might expect the ionized form (corresponding to I_1') to absorb near 443 nm, which corresponds well to the Tt PYP 440 nm intermediate. At this point, we cannot determine whether the hydrogen bond of the chromophore with Tyr42 is present in the 440 nm intermediate (thus corresponding to an ionized form of I_1).

The absorbance of the Tt PYP I_2 intermediate ($\lambda_{max} \sim 368$ nm) decreases at higher pH, as can be seen from the difference absorbance at 358 and 395 nm in Figure 3A. On the other hand, the 440 nm species was not visible below pH 7.5, but becomes dominant above pH 8.5. Note that the amplitude of the I_2 intermediate also decreased in the E46 Hh PYP mutants at higher pH values (*15*). The $I_1'-I_2$ equilibrium in the Hh PYP E46Q mutant has a pK_a of 8.1, while for WT Hh PYP, the pK_a for the $I_1'-I_2$ transition appears to be above 11. Although determining the pK_a for the I_2 to 440 nm transition in Tt PYP is complicated by the occurrence of additional events at even higher pH, we plotted the 395 nm to 440 nm ratios from the difference spectra immediately after illumination versus pH (for the pH range of 6.5−9.1) and fit the curve with a pK_a of 8.6 ($n = 1$, data not shown). This resembles the observed pK_a for the recovery rate at 358 nm (p$K_a = 8.8$), suggesting that ionization of I_2 increases the rate of recovery to the protonated dark-adapted state (P_{BL}). This might seem somewhat surprising at first since the decay of intermediates would involve reprotonation of the chromophore to obtain the 358 nm dark-adapted state. However, a negative charge on the phenolate could facilitate the re-isomerization. As shown in Figure 4, an electron rearrangement from the phenolate oxygen to the carbonyl oxygen can turn the C_7-C_8 double bond into a single bond, which allows a facilitated transition to the trans conformation. Fast protonation of the ionized phenolic oxygen (since we are below the pK_a for ionization of the dark-adapted chromophore of 10.2) leads to the formation of the 358 nm dark-adapted state. It is obvious that such tautomeric structures cannot be formed as readily in the protonated I_2 chromophore, which therefore has a slower recovery. This rationale suggests that (at least at pH 7.0) re-isomerization is the rate-limiting step in the photocycle. As shown with the M100A mutant of Hh PYP, isomerization of the protonated cis chromophore is catalyzed by M100, which accelerates the recovery 1000-fold (*30*). This is presumably due to the ability of the electron-rich M100 sulfur to stabilize the partial positive charge on the aromatic ring of the tautomerized chromophore. Obviously, the effect of M100 is a more significant factor in recovery than the effect of chromophore ionization since the latter is apparent in the M100A mutant, but at all pH values, the recovery is slower than in WT Hh PYP. *Rc. centenaria* PYP also has a slow recovery, which was attributed to a different conformation of the M100-containing loop, where M100 apparently no longer resides over the chromophore in I_2 (*31*). The recovery of *Rc. centenaria* PYP also has a sigmoidal pH dependence similar to those of the Hh PYP M100A mutants (unpublished results). We believe that in Tt PYP, M100 does not facilitate isomerization, presumably due to a different conformation of the M100-containing loop as in the case of *Rc. centenaria* PYP. This would be consistent with the slow recovery kinetics and sigmoidal pH dependence.

Effect of the Equilibrium for Dark-Adapted-State Ionization ($P_{BL}-P$) on the Photocycle. At very high pH values (above approximately pH 9.3), a bleach with an apparent maximum near 490 nm appears in the white light-induced difference spectrum (Figure 3A). The amplitude of the bleach increases with pH. We have already shown above that a pH-dependent dark equilibrium exists, with a pK_a of 10.2, between the two dark-adapted states of Tt PYP (for P_{BL} and P, $\lambda_{max} = 358$ and 465 nm, respectively). Since at pH 10 we have significant amounts of both the 358 and 465 nm forms (Figure 2), it is necessary to determine whether the difference spectrum resulted from a light-induced bleach of the 465 nm form by white light illumination, or solely from dark reactions following the 358 nm bleach. Therefore, we illuminated the Tt PYP with monochromatic 365 nm laser light. Interestingly, when we plotted the difference spectrum (time points after 1 ms) in the 365−520 nm range following 365 nm illumination, we obtained the same spectrum as for white light illumination at the same pH (pH 10 trace in Figure 3A). This suggests that all of the processes observed in the difference spectra are dark reactions resulting from the 358 nm bleach reaction. The kinetic trace at 360 nm (Figure 5A) shows that, besides the expected slow recovery, there is a fast partial recovery (of ~25%) ($\tau = 840$ μs). The slow phase of the recovery kinetics could not be measured accurately with the laser flash instrument since it exceeded the time capacity for detection. However, it appears to be consistent with the measurements in the Cary spectrophotometer after white light illumination (shown in Figure 5B).

The bleach observed at 490 nm after 365 nm excitation (Figures 3A and 6A) could either be due to a photocycle intermediate or to the relaxation of an equilibrium. Since the 490 nm bleach is only observed at pH values where the ionized P species is present (465 nm form), it may be due to a shift in the equilibrium between the 358 and 465 nm species. This implies that the bleach at 490 nm would be the result of a depletion of the 465 nm form. The wavelength maximum of the bleach in the difference spectrum (490 nm) could be shifted to the red due to overlap with the formation of the 440 nm species. A closer look at the difference spectra shows that, when the pH was gradually increased, the 490

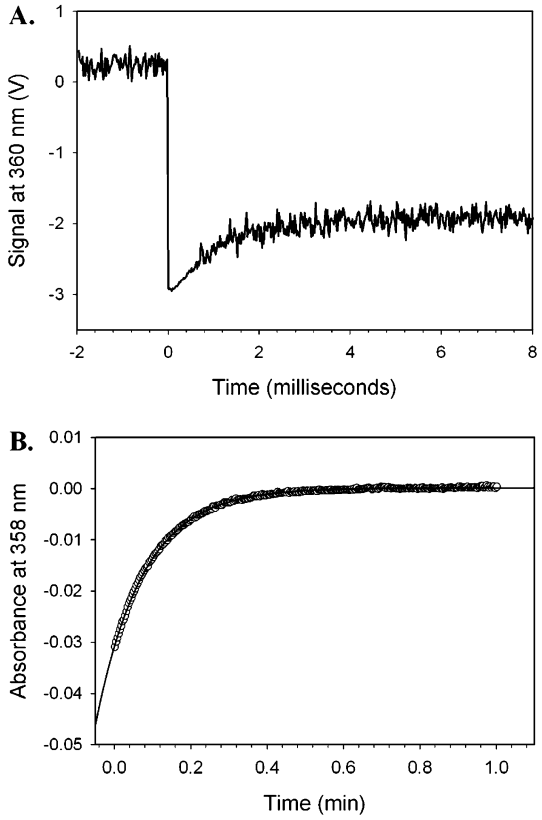

FIGURE 5: Photokinetics at pH 10.0 for WT Tt PYP. (A) Absorbance changes at 360 nm (in arbitrary units) containing bleach and partial recovery during the first 8 ms after 365 nm laser excitation. The partial recovery has a lifetime of 840 μs. (B) Kinetic trace for the slow recovery of WT Tt PYP at 358 nm measured at pH 10.0. The trace was fit with a rate constant of 8.10 min^{-1} (lifetime of 7.41 s).

nm bleach has a maximum around 503 nm at pH 9.3 which is shifted in the difference spectrum toward 490 nm at pH 10, while the 440 nm species shifts its maximum toward 420 nm at pH 10. The shifts in these maxima could be explained by the relative contributions of the formation of the 440 nm species and the depletion of the 465 nm dark-adapted state with changing pH. At pH values around pH 9.0, there is mainly formation of the 440 nm species after a 365 nm light excitation. At higher pH values, the amplitude of the bleach around 490 nm increases with an increase in pH. This makes the maximum of this bleach event shift toward the true maximum of the bleached species (465 nm). In other words, if extrapolated to very high pH values (>11), we expect the 490 nm bleach to shift to 465 nm. Unfortunately, the stability of the sample and hydrolysis of the chromophore does not allow us to perform measurements above pH 10.4.

At all pH values where the 490 nm bleach was present after 365 nm excitation, it appears to have the same slow recovery kinetics as measured at 358 nm [see Table 1; k = 7.54 min^{-1} for the 490 nm recovery at pH 10, compared to k = 8.10 min^{-1} for the 358 nm recovery at the same pH (Figure 6B)]. When the early part of the trace in Figure 6A was fitted, we found that the formation of the apparent 490 nm species at pH 10 has a τ of 210 μs. If the bleach is the result of a shift in the equilibrium between the 358 and 465 nm species, there should be a corresponding increase at 358 nm. We did observe a rapid partial recovery (lifetime of

Table 1: Overview of the Rate Constants Measured at pH 10 after Illumination of Tt PYP with 365 and 445 nm Light

excitation at 365 nm		excitation at 445 nm	
detection wavelength	k (min^{-1})	detection wavelength	k (min^{-1})[a]
358 nm	8.10	370 nm	12.6
440 nm	8.14	440 nm	13.2
490 nm	7.54	490 nm	10.2

[a] The standard deviation error for these values is ~30−40% of the measured value due to the low signal to noise level.

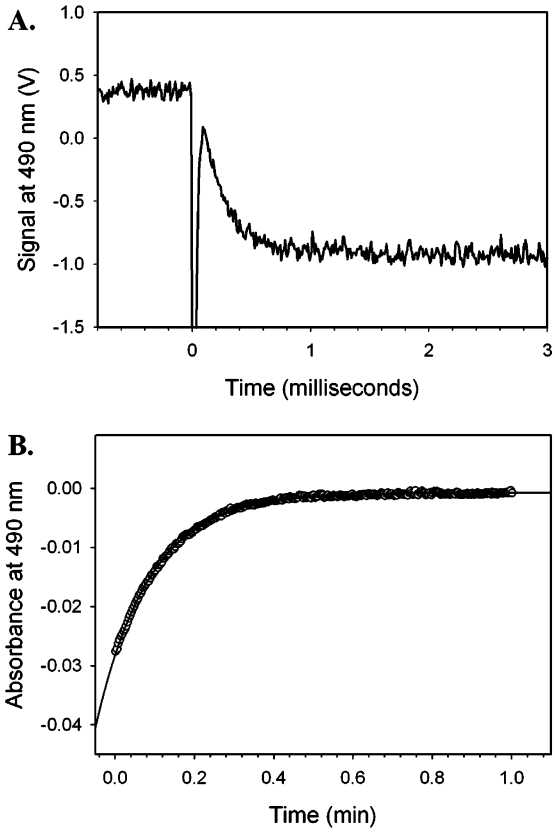

FIGURE 6: Kinetics for WT Tt PYP measured at pH 10.0. (A) Bleach reaction at 490 nm after a 365 nm laser excitation. The bleach occurs with a lifetime of ~210 μs. (B) Kinetic trace for recovery at 490 nm at pH 10.0. The trace could be fit with a rate constant of 7.5 min^{-1} (lifetime of 8 s).

~840 μs; see Figure 5A), but the 4-fold difference in kinetics suggests that the situation is more complex. In addition, the pK_a for the formation of this 490 nm species is almost identical to the pK_a for the pH titration of the dark-adapted state we obtained earlier (pK_a values of 10.5 and 10.2, respectively; data not shown). Thus, we conclude that a change in the dark equilibrium between the two dark-adapted species at high pH (λ_{max} = 358 and 465 nm) is responsible for the 490 nm bleach. As mentioned above, the difference wavelength maximum of the bleached species is markedly shifted because of the admixture with the 440 nm form. Whenever 358 nm light excitation depletes the protonated form by the formation of intermediates, the equilibrium is re-established by rapidly protonating some of the 465 nm form. This can be observed because the transition from the 440 nm form to the dark-adapted state is significantly slower than the relaxation of the dark-adapted-state equilibrium (lifetime of 7.37 s vs ~200 μs at pH 10). The shift in the

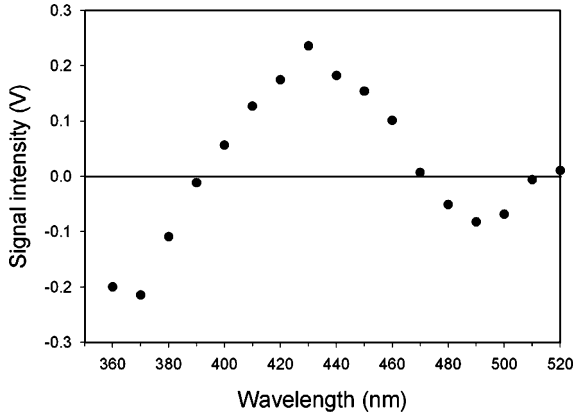

FIGURE 7: Difference spectrum of Tt PYP after 445 nm laser illumination at pH 10. Kinetic traces were collected every 10 nm in the 360−520 nm range, and data points were taken after 5 ms. Because of the high noise level, data points below 360 nm could not be accurately obtained.

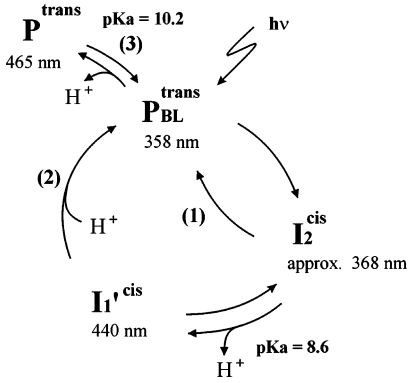

FIGURE 8: Photocycle reactions observed in Tt PYP. Light activation of the dark-adapted state absorbing with a 358 nm maximum (P_{BL}) initiates the formation and recovery of different intermediates, which are in pH-dependent equilibria. The rate and pH dependence of the various reactions are discussed in the text. Absorption maxima are given for each intermediate, and the presumed isomerization state of the chromophore is indicated in superscript.

dark-adapted-state equilibrium also contributes to the observation that the relative amount of bleach at 358 nm after steady-state illumination decreases at higher pH (only approximately 10% bleach at 358 nm after steady-state illumination at pH 10, as compared to 30% at pH 7.0).

Photoactivity of the Ionized Dark State P. Since at pH 10 there is a significant amount of the 465 nm dark-adapted state (P) present, we investigated whether this form was also photoactive and if the P_{BL}−P equilibrium could also be observed after illumination of the 465 nm form. We therefore flashed the sample with 445 and 480 nm laser light. Both wavelengths are expected to excite the 465 nm ionized dark-adapted state (P), without bleaching the 358 nm form (P_{BL}). The difference spectra obtained with 445 and 480 nm illumination were almost identical and have a shape similar to those for 365 nm and white light illumination [compare Figures 3A (pH 10 trace) and Figure 7]. However, the amplitudes of the photoprocesses induced by both 445 and 480 nm excitation are significantly smaller than those after 365 nm excitation (estimated to be ≤1% of the sample absorbance at pH 10). We currently have no explanation for the small amplitudes of these photoprocesses. When the sample was brought back to pH 7.0, the spectrum and kinetics were the same as before the high-pH experiment, indicating that the low quantum yield is not due to degradation of the sample. Nevertheless, the observation of a bleach at both 360 and 490 nm in all the difference spectra indicates that the P_{BL}−P equilibrium of Tt PYP has a similar effect on the photocycle regardless of whether the ionized (P) or protonated (P_{BL}) dark-adapted state is excited. In the case of the 445 and 480 nm excitation, the 465 nm species of the P_{BL}−P equilibrium is depleted, which is replenished from the 358 nm form. This can be observed in the difference spectra as a bleach at 490 and 360 nm. Unfortunately, when the sample was illuminated with 445 and 480 nm light, we could not resolve the kinetics for the P_{BL}−P equilibrium due to the low signal to noise ratio of the kinetic traces.

It appears from the difference spectra that the products of excitation of both P and P_{BL} decay to the same 440 nm intermediate at pH 10 (compare Figures 3A and 7 at pH 10). The rate constants for recovery at 490 and 370 nm and decay at 430 nm after 445 nm excitation are similar (Table 1). Note however that, due to the low signal to noise ratio, these rate constants have large error values. Nevertheless, the rate constants are comparable to the recovery measured after 365 nm excitation and the decay of the 440 nm species at the same pH (presented in the left half of Table 1). This suggests that, at pH 10, both dark-adapted states (P and P_{BL}) form the 440 nm intermediate when illuminated, which decays back to the dark-adapted state mixture with comparable kinetics. Since recovery from the ionized 440 nm species to the protonated P_{BL} involves an additional protonation step of the chromophore, one might expect those kinetics to be slightly different; however, the protonation is a relatively fast process (lifetime between 200 and 800 μs), which cannot be resolved from the slower recovery phase.

A similar relaxation process has recently been shown for the E46Q and E46A mutants of Hh PYP, where the dark-state equilibrium plays a role in the photocycle (*15*). In those cases, the pK_a values for this transition are 4.8 and 7.9, respectively. The equilibrium relaxes on the millisecond time scale as shown by pH jump stopped flow measurements for E46Q (*15*). This equilibrium appears to be slower than in the case of Tt PYP, but the Hh PYP measurements were performed at lower pH (6.3 to 4.8 pH jump) and at lower temperature to slow the photocycle (10 °C). It is important to note that, with the E46 mutants of Hh PYP, both the 365 and 465 nm forms are photoactive, although the 365 nm-initiated photoprocesses have not been studied in detail (*24*).

Overview of the Tt PYP Photocycle. The presumed Tt PYP photocycle, with the different intermediates and pH-dependent equilibria which we described above, is presented in Figure 8. An important difference between this photocycle and the prototypical Hh PYP cycle is that, at pH 7.0, the chromophore in the dark-adapted form of Tt PYP is protonated (P_{BL}). Deprotonation to form P occurs only at higher pH (with a pK_a of 10.2), and is therefore a nonphysiological event and not an essential part of signal-state formation. For clarity, only the photoprocesses initiated by 365 nm illumination are shown in Figure 8. At pH ≤7.0, the only apparent light-induced event is the transition of P_{bl} to I_2 with a very slow recovery (reaction 1). We believe this involves a trans−cis isomerization whereby the chromophore phenolic oxygen remains protonated and therefore resembles the I_2 intermediate of the Hh PYP photocycle. Note that for

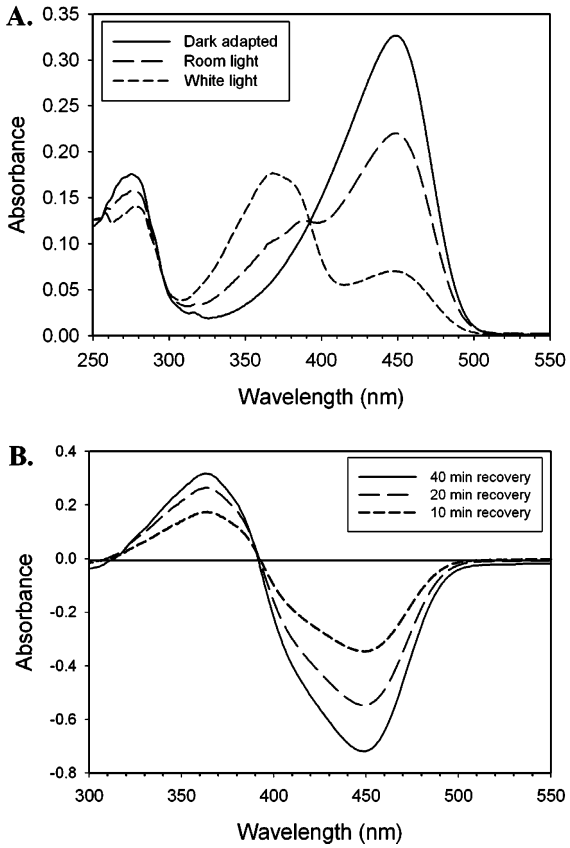

FIGURE 9: (A) Absorption spectra of the *Tc. tepidum* PYP L46E mutant in 20 mM Tris-HCl (pH 7.5). The solid line shows the overnight dark-adapted spectrum; the intermediate spectrum is protein bleached by room light, and the small dashed line is for a sample illuminated for 2 min with white light from a 60 W tungsten lamp. (B) Difference spectrum for L46E recovery. Spectra were taken every 60 s, but only those at 10, 20, and 40 min are shown for clarity. The isosbestic point for the 360 nm to 446 nm transition is at 391 nm. The difference spectrum has shoulders at 410 and 380 nm, and the latter is quite pronounced in the absolute spectrum.

the purposes of this study we did not identify intermediates occurring in a time domain shorter than 100 μs. Above pH 7.5, ionization of intermediates plays an important role, and above pH 8.6, relatively more of the deprotonated 440 nm intermediate than I_2 is formed and the recovery at 358 nm is accelerated ~30-fold from pH 7.0 to 10.0 (reaction 2). The pK_a for this I_2 ionization is ~8.6. We tentatively identify the ionized 440 nm form as I_1', since I_1' was defined in Hh PYP as an intermediate that is in a pH-dependent equilibrium with I_2 (*15*). Above pH 9, there is sufficient ionized form (P) present in the dark (pK_a = 10.2) that relaxation of the dark-state equilibrium ($P-P_{BL}$) has a significant effect on the photocycle. Thus, it partially replenishes the protonated form (P_{BL}) that was photobleached since this process is ~40 times faster than the decay of the 440 nm intermediate at pH 10 (reaction 3). This was seen as a significant bleach around 490 nm and a partial fast recovery phase at 360 nm at pH 10. Note that, at this point, we do not know the degree to which protein conformational changes are involved in any of the transitions of this photocycle.

Characterization of the L46E Mutant of Tc. tepidum PYP. To determine whether E46 would have a similar effect in Tt PYP and Hh PYP, we constructed the L46E mutant. We found that at pH 7.5 it has an absorption peak at 446 nm as in WT Hh PYP (see Figure 9A), but differs in that it also

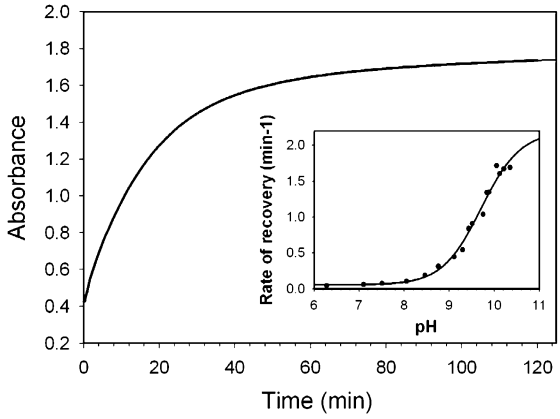

FIGURE 10: Recovery kinetics of L46E at pH 7.0 measured at 440 nm after illumination with white light. The kinetic trace could be fit with a rate constant of 0.066 min^{-1} (lifetime of ~15 min). The inset shows the pH dependence of the recovery rate for the L46E mutant at 446 nm. The plot was fit with a sigmoidal curve with a pK_a of 9.7 (n = 1). Above pH 10.4, significant hydrolysis of the chromophore occurs which impairs further measurement of the recovery rate.

has significant absorbance near 360 nm (with possibly a small shoulder at 380 nm; see below), although the mass spectrum showed that the sample was pure. This was found to be due to steady-state bleaching by room light (~40% is bleached), as in the M100 mutants of Hh PYP (*30*, *32*). Overnight incubation in the dark resulted in elimination of the 360 nm peak and much increased absorbance at 446 nm (Figure 9A, solid line). In contrast, the spectrum of WT Tt PYP did not change significantly when the sample was dark-adapted at 4 °C overnight. The ratio of 280 nm to 446 nm absorbance of dark-adapted L46E was 0.53, comparable to that of WT Hh PYP, which has a similar aromatic amino acid composition. When the dark-adapted sample was illuminated with white light, it was almost completely bleached, but recovered with a lifetime of ~15.1 min at pH 7.0 (Figure 10). This is similar to Hh PYP M100A at pH 7.0 which has a 7.9 min lifetime for recovery. Tt PYP has the M100 residue thought to catalyze cis−trans isomerization of the Hh PYP chromophore and for this reason was expected to have photocycle kinetics like those of WT Hh PYP. However, as mentioned above, the *Rc. centenaria* PYP domain (Rc PYP) has a different conformation in the region of M100 as seen by X-ray studies (*31*), which could be responsible for the slow recovery of that protein (~3 min). In Tt PYP, most residues in this loop are the same as in *Rc. centenaria* PYP (see the sequence comparison in ref *9*), which is consistent with the interpretation that an altered loop conformation slows recovery, although there could be other explanations as well.

It is known that Hh PYP, N-terminally truncated by 6, 15, or 23 residues, also has progressively slower recovery kinetics than the native or WT protein (*33*). Mass spectrometry before and after illumination and recovery of Tt PYP shows that the protein is intact. The N-terminal pair of helices is held tightly against the remainder of the protein by hydrophobic interactions. Therefore, substitution or mutagenesis of hydrophobic residues in the N-terminal segment should have effects comparable to those of truncation. From comparison of PYP amino acid sequences, it is apparent that F6 is conserved in all PYPs except for Tt PYP, which has an F6A substitution. However, a single substitution may not

be sufficient to slow the recovery by as much as we observe since, for example, the Δ1−6 Hh PYP has a lifetime of 26 s for recovery as compared to a lifetime of 160 ms for WT Hh PYP. Tt PYP also has an I11A substitution, which, in combination with the F6A substitution, may be responsible in part for our results considering that the Δ1−15 Hh PYP has a lifetime of 7 min. Rc PYP has only an F28V substitution that might slow recovery, consistent with somewhat faster recovery than for Tt PYP. Therefore, it is likely that the slow recovery kinetics in Tt and Rc PYPs may be due to a combination of altered M100 conformation and substitution of hydrophobic residues at the interface between the N-terminus and the remainder of the protein.

Interestingly, the difference spectrum for L46E recovery (Figure 9B) shows that in addition to the expected bleaching of the 446 nm absorbing species and formation of the 360 nm absorbing form (with isosbestic at 391 nm), there seems to be 410 and 380 nm shoulders. The origin of these two spectral shoulders is not yet clear, but it is intriguing that in the difference spectrum of *Rb. capsulatus* PYP, although on a much faster time scale, there was also the observation of bleaching of a 410 nm component (*19*).

When studying the effect of pH on the recovery of the L46E mutant of Tt PYP, we found that, in contrast to the bell-shaped pH dependence of WT Hh PYP with pK_a values of 6.4 and 9.4, there is a sigmoidal pH dependence in the pH 6−10.4 range, governed by a pK_a of ∼9.7 (see the inset of Figure 10). Note that, although most kinetics experiments with L46E were performed with white light, some pH data points (pH 7.0, 7.5, and 9.5) were repeated with >410 nm light to exclude illumination of the 360 nm form, and the same kinetic values were obtained as with white light illumination. The sigmoidal pH dependence is similar to that observed with all M100 and E46 mutants of Hh PYP (*15*, *24*, *25*, *30*, *32*). It was earlier suggested that the pK_a of 6.4 in WT Hh PYP is due to protonation/deprotonation of E46 and that at 9.4 is due to the chromophore when exposed to solvent in the photobleached protein (*34*). Thus, either the negative charge on E46 or that on the chromophore, but not both at once, accelerates recovery in WT Hh PYP and the E46 mutants. However, this does not explain the pH dependence of the M100 mutants, which are characterized by very slow recoveries like Rc and Tt PYPs. In the case of Tt PYP, we can presume that the pK_a of 9.7 is due to deprotonation of the phenolic hydroxyl group of the chromophore in the photobleached form, since it is similar to the pK_a of the free chromophore (pK_a = 9). This again implies that the anionic form of the chromophore returns to the dark-adapted conformation faster than the protonated form, which can be explained by a facilitated isomerization of the tautomeric structure. This effect can be observed only when the cis−trans catalyzing properties of M100 are absent. Although the introduction of E46 in Tt PYP has a significant spectral effect, it does not restore the bell-shaped pH dependence as observed in Hh PYP, but rather resembles the M100 mutants, which is in agreement with the proposed different conformation of M100 in Tt PYP as discussed above.

Conclusions. We have characterized the *Tc. tepidum* PYP domain and have shown that the pH 7.0 form of Tt PYP, which has an absorption maximum at 358 nm, is in equilibrium with a higher-pH form absorbing around 465 nm (pK_a = 10.2) similar to the dark-adapted-state equilibria of E46 mutants of Hh PYP (which have significantly lower pK_a values). We have also shown that the 358 nm form is photoactive, and that the long-lived photobleached form (I_2) is in a pH-dependent equilibrium with a further red-shifted intermediate (λ_{max} ∼ 440 nm), comparable to the Hh PYP $I_1'-I_2$ equilibrium. The photocycle of Tt PYP is very slow compared to that of Hh PYP (3 orders of magnitude slower at pH 7.0) which is presumably related to a different functional role. The slower recovery times and sigmoidal pH dependence of the recovery suggest that the M100 side chain does not catalyze the cis−trans dark re-isomerization, resembling the closest homologue, the *Rc. centenaria* PYP domain.

Since this is the only WT PYP that has been found so far which is lacking the important E46 residue, we also investigated the L46E mutant and found it to have an absorption spectrum and kinetics similar to those of the M100 mutants of the prototypical Hh PYP. Three-dimensional structures for both WT Tt PYP and L46E should reveal the presumed structural differences with Hh PYP.

ACKNOWLEDGMENT

We thank Maarten P. Heyn for his critical reading and helpful suggestions.

REFERENCES

1. Meyer, T. E. (1985) Isolation and characterization of soluble cytochromes, ferredoxins and other chromophoric proteins from the halophilic phototrophic bacterium *Ectothiorhodospira halophila*, *Biochim. Biophys. Acta 806*, 175−183.
2. Meyer, T. E., Yakali, E., Cusanovich, M. A., and Tollin, G. (1987) Properties of a water-soluble, yellow protein isolated from a halophilic phototrophic bacterium that has photochemical activity analogous to sensory rhodopsin, *Biochemistry 26*, 418−423.
3. Jiang, Z. Y., Swem, L. R., Rushing, B. G., Devanathan, S., Tollin, G., and Bauer, C. E. (1999) Bacterial photoreceptor with similarity to photoactive yellow protein and plant phytochromes, *Science 285*, 406−409.
4. Pellequer, J., Wager-Smith, K. A., Kay, S. A., and Getzoff, E. D. (1998) Photoactive yellow protein: A structural prototype for the three-dimensional fold of the PAS domain superfamily, *Proc. Natl. Acad. Sci. U.S.A. 95*, 5884−5890.
5. Cusanovich, M. A., and Meyer, T. E. (2003) Photoactive yellow protein: A prototypic PAS domain sensory protein and development of a common signaling mechanism, *Biochemistry 42*, 4759−4770.
6. Taylor, B. L., and Zhulin, I. B. (1999) PAS domains: Internal sensors of oxygen, redox potential, and light, *Microbiol. Mol. Biol. Rev. 63*, 479−506.
7. Gong, W., Hao, B., Mansy, S. S., Gonzales, G., Gilles-Gonzales, M. A., and Chan, M. K. (1998) Structure of a biological oxygen sensor: A new mechanism for heme-driven signal transduction, *Proc. Natl. Acad. Sci. U.S.A. 95*, 15177−15182.
8. Cabral, J. H. M., Lee, A., Cohen, S. L., Chait, B. T., Li, M., and Mackinnon, R. (1998) Crystal structure and functional analysis of the HERG potassium channel N-terminus: A eukaryotic PAS domain, *Cell 95*, 649−655.
9. Kyndt, J. A., Meyer, T. E., and Cusanovich, M. A. (2004) Photoactive yellow protein, bacteriophytochrome, and sensory rhodopsin in purple phototrophic bacteria, *Photochem. Photobiol. Sci. 3*, 519−530.
10. Meyer, T. E., Fitch, J. C., Bartsch, R. G., Tollin, G., and Cusanovich, M. A. (1990) Soluble cytochromes and a photoactive yellow protein isolated from the moderately halophilic purple phototrophic bacterium, *Rhodospirillum salexigens*, *Biochim. Biophys. Acta 1016*, 364−370.
11. Koh, M., Van Driessche, G., Samyn, B., Hoff, W. D., Meyer, T. E., Cusanovich, M. A., and Van Beeumen, J. J. (1996) Sequence evidence for strong conservation of the photoactive yellow proteins

from the halophilic phototrophic bacteria *Chromatium salexigens* and *Rhodospirillum salexigens*, *Biochemistry 35*, 2526−2534.
12. Ujj, L., Devanathan, S., Meyer, T. E., Cusanovich, M. A., Tollin, G., and Atkinson, G. H. (1998) New photocycle intermediates in the photoactive yellow protein from *Ectothiorhodospira halophila*: Picosecond transient absorption spectroscopy, *Biophys. J. 75*, 406−412.
13. Devanathan, S., Pacheco, A., Ujj, L., Cusanovich, M. A., Tollin, G., Lin, S., and Woodbury, N. (1999) Femtosecond spectroscopic observations of initial intermediates in the photocycle of the photoactive yellow protein from *Ectothiorhodospira halophila*, *Biophys. J. 77*, 1017−1023.
14. Borucki, B., Devanathan, S., Otto, H., Cusanovich, M. A., Tollin, G., and Heyn, M. P. (2002) Kinetics of proton uptake and dye binding by photoactive yellow protein in WT and in the E46Q and E46A mutants, *Biochemistry 41*, 10026−10037.
15. Borucki, B., Otto, H., Joshi, C. P., Cusanovich, M. A., Devanathan, S., Tollin, G. and Heyn, M. P. (2003) pH dependence of the photocycle kinetics of the E46Q mutant of photoactive yellow protein: Protonation equilibrium between I_1 and I_2 intermediates, chromophore deprotonation by hydroxyl uptake, and protonation relaxation of the dark state, *Biochemistry 42*, 8780−8790.
16. Xie, A., Kelemen, L., Hendriks, J., White, B. J., Hellingwerf, K. J., and Hoff, W. D. (2001) Formation of a new buried charge drives a large-amplitude protein quake in photoreceptor activation, *Biochemistry 40*, 1510−1517.
17. Kort, R., Hoff, W. D., Van West, M., Kroon, A. R., Hoffer, S. M., Vlieg, K. H., Crielaard, W., Van Beeumen, J. J., and Hellingwerf, K. J. (1996) The xanthopsins: A new family of eubacterial blue-light photoreceptors, *EMBO J. 15*, 3209−3218.
18. Haker, A., Hendriks, J., Gensch, T., Hellingwerf, K., and Crielaard, W. (2000) Isolation, reconstitution and functional characterization of the *Rhodobacter sphaeroides* photoactive yellow protein, *FEBS Lett. 486*, 52−56.
19. Kyndt, J. A., Hurley, J. K., Devreese, B., Meyer, T. E., Cusanovich, M. A., Tollin, G., and Van Beeumen, J. J. (2004) *Rhodobacter capsulatus* photoactive yellow protein: Genetic context, spectral and kinetics characterization, and mutagenesis, *Biochemistry 43*, 1808−1820.
20. Madigan, M. T. (1986) *Chromatium tepidum* sp. nov., a thermophilic photosynthetic bacterium of the family *Chromatiaceae*, *Int. J. Syst. Bacteriol. 36*, 222−227.
21. Kyndt, J. A., Vanrobaeys, F., Fitch, J. C., Devreese, B. V., Meyer, T. E., Cusanovich, M. A., and Van Beeumen, J. J. (2003) Heterologous production of *Halorhodospira halophila* holophotoactive yellow protein through tandem expression of the postulated biosynthetic genes, *Biochemistry 42*, 965−970.
22. Simondsen, R. P., and Tollin, G. (1983) Transient kinetics of redox reactions of flavodoxin: Effects of chemical modification of the flavin mononucleotide prosthetic group on the dynamics of intermediate complex formation and electron transfer, *Biochemistry 22*, 3008−3016.
23. Borgstahl, G. E. O., Williams, D. R., and Getzoff, E. D. (1995) 1.4 Å structure of photoactive yellow protein, a cytosolic photoreceptor: Unusual fold, active site, and chromophore, *Biochemistry 34*, 6278−6287.
24. Devanathan, S., Brudler, R., Hessling, B., Woo, T. T., Gerwert, K., Getzoff, E. D., Cusanovich, M. A., and Tollin, G. (1999) Dual photoactive species in Glu46Asp and Glu46Ala mutants of photoactive yellow protein: A pH driven color transition, *Biochemistry 38*, 13766−13772.
25. Genick, U. K., Devanathan, S., Meyer, T. E., Canestrelli, I. L., Williams, E., Cusanovich, M. A., Tollin, G., and Getzoff, E. D. (1997) Active site mutants implicate key residues for control of color and light cycle kinetics of photoactive yellow protein, *Biochemistry 36*, 8−14.
26. Hendriks, J., van Stokkum, I. H. M., Crielaard, W., and Hellingwerf, K. J. (1999) Kinetics of and intermediates in a photocycle branching reaction of the photoactive yellow protein from *Ectothiorhodospira halophila*, *FEBS Lett. 458*, 252−256.
27. Joshi, C. P., Borucki, B., Otto, H., Meyer, T. E., Cusanovich, M. A., and Heyn, M. P. (2005) Photoreversal kinetics of the I_1 and I_2 intermediates in the photocycle of photoactive yellow protein by double flash experiments with variable time-delay, *Biochemistry 44*, 656−665.
28. Anderson, S., Crosson, S., and Moffat, K. (2004) Short hydrogen bonds in photoactive yellow protein, *Acta Crystallogr. D60*, 1008−1016.
29. Kort, R., Vonk, H., Xu, X., Hoff, W. D., Crielaard, W., and Hellingwerf, K. J. (1996) Evidence for *trans-cis* isomerization of the p-coumaric acid chromophore as the photochemical basis of the photocycle of photoactive yellow protein, *FEBS Lett. 382*, 73−78.
30. Devanathan, S., Genick, U. K., Canestrelli, I. L., Meyer, T. E., Cusanovich, M. A., Getzoff, E. D., and Tollin, G. (1998) New insights into the photocycle of *Ectothiorhodospira halophila* photoactive yellow protein: Photorecovery of the long-lived photobleached intermediate in the Met100Ala mutant, *Biochemistry 37*, 11563−11568.
31. Rajagopal, S., and Moffat, K. (2003) Crystal structure of a photoactive yellow protein from a sensor histidine kinase: Conformational variability and signal transduction, *Proc. Natl. Acad. Sci. U.S.A. 100*, 1649−1654.
32. Kumauchi, M., Hamada, N., Sasaki, J., and Tokunaga, F. (2002) A role of methionine100 in facilitating PYP_M decay process in the photocycle of photoactive yellow protein, *J. Biochem. 132*, 205−210.
33. Harigai, M., Yasuda, S., Imamoto, Y., Yoshihara, K., Tokunaga, F., and Kataoka, M. (2001) Amino acids in the N-terminal region regulate the photocycle of photoactive yellow protein, *J. Biochem. 130*, 51−56.
34. Meyer, T. E., Devanathan, S., Woo, T., Getzoff, E. D., Tollin, G., and Cusanovich, M. A. (2003) Site specific mutations provide new insights into the origin of pH effects and alternative spectral forms in the photoactive yellow protein from *Ectothiorhodospira halophila*, *Biochemistry 42*, 3319−3325.

BI047373N